Isotopes of nitrogen on Mars: Atmospheric measurements by Curiosity's mass spectrometer

Michael H. Wong,[1,2] Sushil K. Atreya,[1] Paul N. Mahaffy,[3] Heather B. Franz,[3] Charles Malespin,[3] Melissa M. Trainer,[3] Jennifer C. Stern,[3] Pamela G. Conrad,[3] Heidi L.K. Manning,[4] Robert O. Pepin,[5] Richard H. Becker,[5] Christopher P. McKay,[6] Tobias C. Owen,[7] Rafael Navarro-González,[8] John H. Jones,[9] Bruce M. Jakosky,[10] and Andrew Steele[11]

The Sample Analysis at Mars (SAM) instrument suite on the Mars Science Laboratory (MSL) measured a Mars atmospheric $^{14}N/^{15}N$ ratio of 173 ± 11 on sol 341 of the mission, agreeing with Viking's measurement of 168 ± 17 [*Nier and McElroy*, 1977]. The MSL/SAM value was based on Quadrupole Mass Spectrometer (QMS) measurements of an enriched atmospheric sample, with CO_2 and H_2O removed. Doubly-ionized nitrogen data at m/z 14 and 14.5 had the highest signal/background ratio, with results confirmed by m/z 28 and 29 data.

Gases in SNC meteorite glasses have been interpreted as mixtures containing a martian atmospheric component [*Bogard and Johnson*, 1983], based partly on distinctive $^{14}N/^{15}N$ and $^{40}Ar/^{14}N$ ratios [*Becker and Pepin*, 1984]. Recent MSL/SAM measurements of the $^{40}Ar/^{14}N$ ratio (0.51 ± 0.01) are incompatible with the Viking ratio (0.35 ± 0.08) [*Mahaffy et al.*, 2013]. The meteorite mixing line is more consistent with the atmospheric composition measured by Viking than by MSL.

1. Introduction

Isotope ratios are excellent tracers of atmospheric source and loss processes over planetary timescales. In the case of martian oxygen and carbon, atmospheric evolution models must account for the exchange between atmospheric and surface/subsurface reservoirs [*Jakosky*, 1991; *Webster et al.*, 2013]. The potential for exchange of nitrogen between the atmosphere and surface of Mars is not currently understood, but such exchange would be very important to the study of martian habitability that is the focus of the MSL mission [*Grotzinger et al.*, 2012].

The atmospheric nitrogen isotopic ratio is difficult to measure. Very weak absorption lines are produced by the dipole forbidden vibrational-rotational transitions of ground state N_2, so the spectroscopic techniques used to measure isotope ratios in other molecules cannot be applied to molecular nitrogen. Of the 10 science instruments of the MSL payload [*Grotzinger et al.*, 2012], SAM's mass spectrometer provides the best capability to measure the nitrogen isotopic ratio [*Mahaffy et al.*, 2012]. Independent measurements of $^{14}N/^{15}N$ were conducted by mass spectrometers on Viking lander 2 [*Owen et al.*, 1977; *Owen*, 1992] and the two Viking lander aeroshells [*Nier and McElroy*, 1977]. The surface and descent measurements found $^{14}N/^{15}N$ of 170 ± 15 and 168 ± 17, respectively.

2. Experiments

SAM is a highly capable and configurable instrument suite for analyzing gases either directly sampled from the atmosphere, or evolved from solid samples [*Mahaffy et al.*, 2012]. SAM/QMS determines isotopic ratios based on ratios of detector counting rates. In direct atmospheric experiments, CO^+ ions (from CO_2) interfere at m/z 28 and 29 (where the N_2^+ parent ions are detected). But there is no CO^{++} contribution at m/z 14, so we can derive $^{14}N/^{15}N$ from direct atmospheric experiments using the m/z 14/14.5 count ratio. In enrichment experiments, chemical scrubbers remove CO_2, H_2O, and other species with chemical affinity to the scrubber material. The enrichment process allows determination of the isotopic ratio using m/z 28/29 and 14/29 count ratios. We further boost signal level (compared to the normal dynamic mode) using a semi-static mode, where the pumping rate out of the QMS is reduced. Figure 1 shows a mass spectrum from an enrichment experiment in dynamic mode, spanning the relevant m/z range for nitrogen analysis.

On Jupiter, the nitrogen isotopic ratio was determined using Galileo Probe Mass Spectrometer measurements of NH_3^{++}, to avoid interferences at m/z 17 and 18 from water [*Owen*, 2001; *Wong et al.*, 2004]. We use a similar approach in the MSL/SAM analysis, although there is an additional complication because the count ratio of m/z 14/14.5 includes contributions from two nitrogen daughter ions, N^+ and N_2^{++}.

To extract the nitrogen isotopic ratio, we first measure a splitting fraction (derived from SAM QMS pre-flight calibration data) that gives the relative contributions from these two daughter ions:

$$\beta = \frac{N^+}{N^+ + N_2^{++}} = \frac{2\left[\frac{m14}{m14.5}\right] - {}^{14}N/{}^{15}N}{2\left[\frac{m14}{m14.5}\right] + 1}, \qquad (1)$$

[1]Department of Atmospheric, Oceanic, and Space Sciences, University of Michigan, Ann Arbor MI, USA.
[2]Astronomy Department, University of California, Berkeley CA, USA.
[3]Code 699, NASA Goddard Space Flight Center, Greenbelt MD, USA.
[4]Concordia College, Moorhead MN, USA.
[5]University of Minnesota, Minneapolis MN, USA.
[6]NASA Ames Research Center, Moffet Field CA, USA.
[7]University of Hawai'i, Honolulu HI, USA.
[8]Universidad Nacional Autónoma de México, México City, México.
[9]NASA Johnson Space Center, Houston TX, USA.
[10]LASP, University of Colorado, Boulder CO, USA.
[11]Geophysical Laboratory, Carnegie Institution of Washington, Washington, DC, USA.

Copyright 2013 by the American Geophysical Union.
0094-8276/13/$5.00

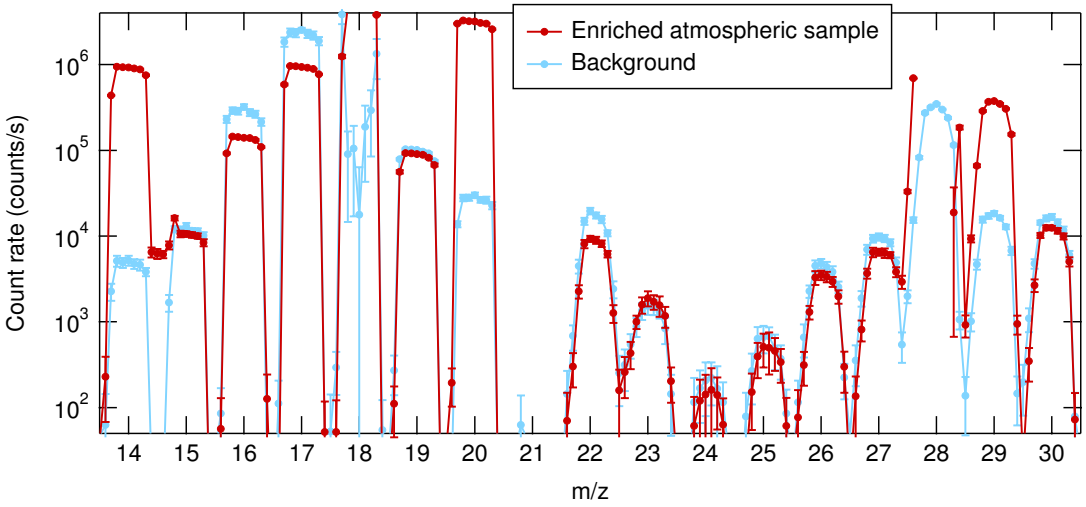

Figure 1. High-resolution mass spectrum from the enrichment experiment on sol 232. Sample spectrum is an average of data from enrichment cycle 9 (see Fig. 2). Nitrogen ions are present at m/z 14, 14.5, 28, and 29. The singly-ionized N_2 "parent ion" appears in the Mars data at m/z 28 (for $^{14}N^{14}N$) and at m/z 29 (for $^{15}N^{14}N$). A third parent ion, $^{15}N^{15}N$, is so rare as to produce no signal above the background level (difference between red and blue curves). For a comparison of the m/z 14–15 range in the direct atmospheric experiment, see *Wong et al.* [2013].

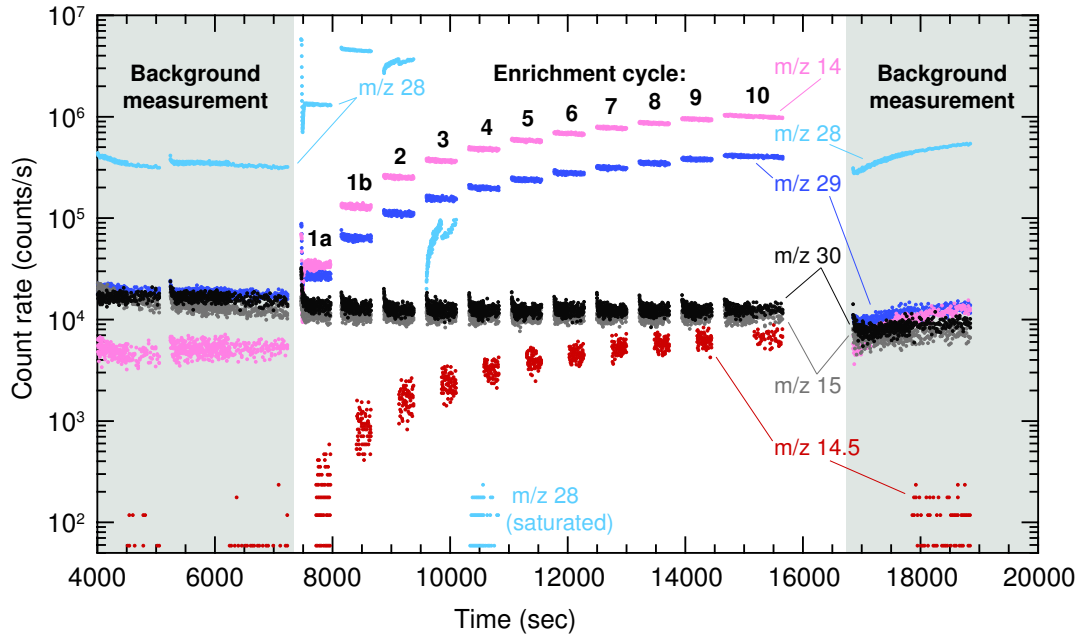

Figure 2. Visual narrative of the sol 232 enrichment experiment. Parent and daughter nitrogen ions are shown as colored points. Background measurements (shaded) are used to characterize the background signal that must be subtracted from the data before calculating count ratios. Detector corrections have been applied to the data (see Supplemental Material). In each of ten enrichment cycles, an atmospheric sample was introduced, and CO_2 and H_2O were removed by chemical scrubbers [*Mahaffy et al.*, 2012]. The enriched sample from one cycle was then combined with a new injection of Mars atmosphere and scrubbed to produce the next sample. Signal at m/z 28 decreases in enrichment cycle 2 and later due to detector saturation at high source pressures.

where the count rates at a mass/charge ratio of m/z X are represented as mX, and the $^{14}N/^{15}N$ is independently measured in the calibration gas. We find $\beta = 0.404 \pm 0.033$ based on five experiments [*Wong et al.*, 2013]. The $^{14}N/^{15}N$ isotopic ratio is then derived from the splitting fraction β and the flight m/z 14/14.5 count ratio (see supplementary material):

$$^{14}N/^{15}N = 2(1-\beta)\left[\frac{\mathrm{m14}}{\mathrm{m14.5}}\right] - \beta. \quad (2)$$

Additional count ratios can be used to measure nitrogen isotopes in the enrichment experiments. Measurement of the $^{14}N/^{15}N$ ratio directly from the parent ions is difficult

Table 1. Mars nitrogen isotopic ratios measured in atmospheric N_2

MSL Sol[a]	$^{14}N/^{15}N$	$\delta^{15}N$ (‰)[b]	Count ratio	Limiting S/BG[c]	Experiment type
341 (night)	173 ± 11	572 ± 82	m14/m14.5	≤ 388	Enrichment (MSL/SAM, semi-static MS)
341 (night)	175 ± 21	554 ± 187	m28/m29	3.4	Enrichment (MSL/SAM, semi-static MS)
232 (night)	178 ± 12	528 ± 103	m14/m14.5	≤ 97	Enrichment (MSL/SAM, dynamic MS)
232 (night)	179 ± 11	519 ± 91	m28/m29	≤ 13	Enrichment (MSL/SAM, dynamic MS)
19 (night)	150 ± 60	813 ± 725	m14/m14.5	2	Direct atmospheric (MSL/SAM)
45 (night)	151 ± 27	798 ± 324	m14/m14.5	9	Direct atmospheric (MSL/SAM)
77 (night)	169 ± 19	611 ± 183	m14/m14.5	8	Direct atmospheric (MSL/SAM)
278 (day)	173 ± 27	572 ± 245	m14/m14.5	14	Direct atmospheric (MSL/SAM)
284 (night)	172 ± 38	582 ± 345	m14/m14.5	17	Direct atmospheric (MSL/SAM)
292 (night)	177 ± 14	537 ± 123	m14/m14.5	20	Direct atmospheric (MSL/SAM)
321 (day)	167 ± 14	628 ± 140	m14/m14.5	12	Direct atmospheric (MSL/SAM)
Testbed[d]	270 ± 28	8 ± 104	m14/m14.5	≤ 33	Testbed enrichment TID 50765
Comparison measurements					
Viking aeroshell MS	168 ± 17	619 ± 182	m28/m29	< 50	Viking, 125 km [*Nier and McElroy*, 1977]
Viking lander MS	165 ± 17	649 ± 183	m28/m29?[e]	?[e]	Viking, surface [*Owen et al.*, 1977]
Viking lander MS	170 ± 15	600 ± 155	m28/m29?[e]	?[e]	Viking, surface [*Owen*, 1992]

[a] MSL landing occurred on sol 0 at 15:03 local mean solar time, or UTC 2012-08-06 05:17.

[b] $\delta^{15}N$ (‰) $= 1000(R/R_{AIR} - 1)$, where $R = {}^{15}N/{}^{14}N$ in the sample, and $R_{AIR} = 0.003676$ [*Coplen et al.*, 2002].

[c] Signal to background level (S/BG) is "limiting" because it refers to the count rate with the poorest S/BG (e.g., m/z 14 in the case of the m/z 14/14.5 ratio). The "≤" symbol means that the S/BG level changes over the course of the experiment, and the best S/BG ratio over the full experiment range is reported.

[d] Testbed experiment is listed to confirm SAM accuracy with a gas sample of known isotopic composition ($\delta^{15}N = 0$‰, $^{14}N/^{15}N = 272$). Analysis method is the same as for flight data.

[e] Viking lander MS publications do not describe count ratios used for isotopic determination, or S/BG levels in the data. Experiments used enriched atmospheric samples.

because the signal level is very high at m/z 28 over most of the enrichment experiment; in fact Fig. 2 shows that the m/z 28 signal is near saturation in the first enrichment cycle (labeled 1a and 1b). The m/z 28 counting rate decreases in enrichment cycles 2–4 due to saturation, with 0 counts/s in the subsequent cycles. The isotope ratio can also be derived from m/z 14/29 data, but different voltage frequencies used above and below m/z 20 [*Mahaffy et al.*, 2012] introduce complications that have not yet been fully resolved.

3. Results

Table 1 lists nitrogen isotopic results from SAM up through MSL sol 360 (PDS release 4). Uncertainties include all sources of error (see Supplemental Material). Specifically, we include uncertainties from detector corrections, background subtraction, statistical noise, and splitting fractions. SAM background corrections are significant, so the limiting S/BG level is listed as a measure of the confidence in each measurement. Ions containing ^{15}N are less abundant than those containing only ^{14}N, so the limiting S/BG ratio corresponds to the heavy nitrogen term in the ratio. Where known, S/BG levels from other instruments are also given for comparison.

The most reliable MSL/SAM measurement of $^{14}N/^{15}N$ comes from m/z 14/14.5 in the semi-static enrichment experiment, where a S/BG ratio of 388 was achieved. Results at low S/BG have much more scatter than results at S/BG > 50 (see supplementary material), suggesting that imperfect background corrections dominate the uncertainty in the direct atmospheric measurements. The largest single source of uncertainty in the isotopic ratio is the uncertainty in β (Eqn. 1 and Fig. S1). The range of $^{14}N/^{15}N$ ratios derived from MSL/SAM data falls completely within the error bars of Viking measurements.

4. Discussion

Non-terrestrial nitrogen isotopic ratios in martian meteorite samples have been interpreted as tracers of atmospheric gas, trapped within the meteorites at their time of ejection from Mars. Figure 3 compares laboratory analyses of gases evolved from meteorite samples to in situ measurements of the Mars atmosphere by Viking and MSL. Selected step-heating gas releases in the terrestrial laboratory experiments can be used to define mixing lines between the compositional measurements. The choice of steps for analysis (black symbols, and references in figure caption) was intended to eliminate contributions from terrestrial air or organic contamination. For comparison, we also show meteorite data (red symbols) and linear fits based on the total gas released in each experiment. These total gas release data are free from uncertainties introduced by subjective interpretation of stepped heating data. The mixing line slope is not significantly affected by uncertainties in cosmic ray exposure ages [*Nyquist et al.*, 2001; *Schwenzer et al.*, 2007].

There is a clear disagreement between the Ar/N measurement by MSL/SAM of 0.51 ± 0.01 [*Mahaffy et al.*, 2013] and by multiple Viking instruments of 0.35 ± 0.08 [*Oyama and Berdahl*, 1977]. All of the meteorite mixing lines are consistent with Viking composition and inconsistent with MSL.

Three possible explanations for the disagreements can be considered: that the MSL composition is wrong, that the Viking composition is wrong, or that the martian atmospheric composition is variable. Internal and peer reviews of the MSL/SAM data argue against the first possibility at this time [*Mahaffy et al.*, 2013]. Similarly, the Viking composition seems highly robust, with good agreement among multiple instruments. The MSL $^{14}N/^{15}N$ ratio falls easily within the error bars of the Viking measurements by both lander and aeroshell mass spectrometer experiments. So the primary disagreement is with the Ar/N ratio. This ratio was repeatedly measured by both the Viking lander mass spectrometer [*Owen et al.*, 1977] and the gas exchange experiment [*Oyama and Berdahl*, 1977]. Unfortunately, Viking

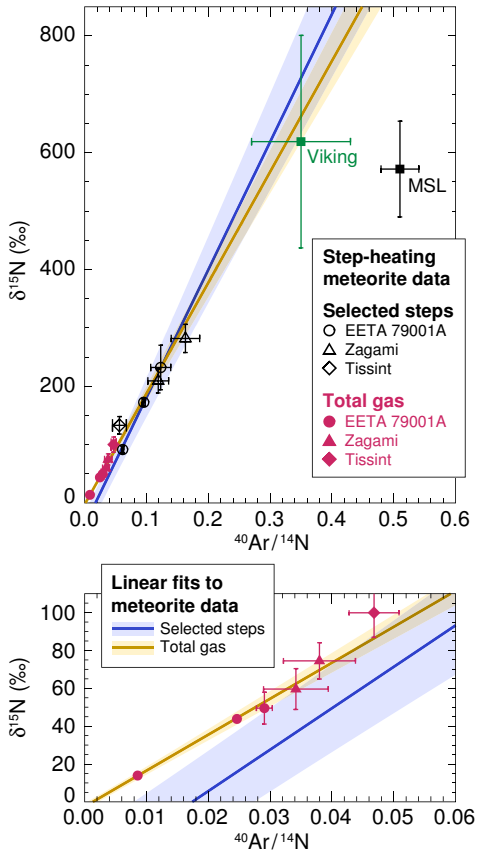

Figure 3. Pseudo-three-isotope plots at two different magnifications (comparing ^{14}N, ^{15}N, and ^{40}Ar) showing Mars meteorite and atmosphere measurements and linear fits. The meteorite data suggest mixing between at least two components: martian atmosphere and terrestrial atmosphere. Black meteorite data include only selected temperature steps in stepped-heating gas release experiments. Red data points include the total gas released at all temperatures. Meteorite data are from *Becker and Pepin* [1984, EETA 79001A samples C1 and C2], *Wiens et al.* [1986, sample C3], *Marti et al.* [1995, Zagami], *Chennoui Aoudjehane et al.* [2012, Tissint] and *Avice* [2012, Tissint]. Viking Ar/N ratio is from *Oyama and Berdahl* [1977], and Viking δ^{15}N is from *Nier and McElroy* [1977]. MSL values are from SAM/QMS measurements, with δ^{15}N described in this work and Ar/N from *Mahaffy et al.* [2013]. Linear fits included uncertainties in both Ar/N and δ^{15}N, following the method of *York et al.* [2004], assuming uncorrelated errors.

flight data are no longer available, so we cannot repeat the same validation we applied to the MSL data. Therefore, the possibility that Viking Ar/N measurements were erroneous can only be speculation.

There is currently no satisfactory mechanism that could explain a variable Ar/N ratio in the martian atmosphere. Adsorbed CO_2 and H_2O in the regolith make up a large volatile reservoir that exchanges over time with the atmosphere and polar caps [e.g., *Fanale et al.*, 1982; *Fanale and Jakosky*, 1982]. Nitrogen and argon are not thought to participate in this cycle, although these gases do adsorb onto martian soil [*Ballou et al.*, 1978]. A previously unknown surface-atmosphere exchange mechanism would need to involve very large column density changes: a release of up to 1 kg m^{-2} Ar or sequestration of up to 0.7 kg m^{-2} N_2, prior to 2012. Column density changes might be thermally driven by global warming of 0.65 K since Viking [*Fenton et al.*, 2007], or related to a reduction of polar cap mass [*Malin et al.*, 2001], but MSL measurements from early spring to late summer on Mars do not support any variation in Ar/N [*Atreya et al.*, 2013; *Trainer et al.*, 2013].

Table 2. Solar system nitrogen isotopic ratios

Measurement	^{14}N/^{15}N	δ^{15}N (‰)	Reference
Protosolar/primordial			
Sun (Genesis)	441 ± 5	–383 ± 8	*Marty et al.* [2011]
Jupiter	434 ± 7.5	–373 ± 11	*Owen* [2001]
ISM	450 ± 98	–395 ± 168	*Dahmen et al.* [1995]
Secondary atmospheres			
Mars (MSL)	173 ± 11	572 ± 82	(this work)
Titan	183 ± 5	487 ± 42	*Niemann et al.* [2005]
Venus	272 ± 54	0 ± 250	*Hoffman et al.* [1979]
Earth	272	0	

Heavy nitrogen in the atmosphere of Mars is enriched relative to both the protosolar isotopic ratio and the ratio in the terrestrial and venusian atmospheres (Table 2), as well as to the primordial Mars atmosphere as suggested by the meteorite ALH84001 with $\delta^{15}N = 4 \pm 2$ ‰ [*Marti and Mathew*, 2000]. The enrichment of ^{15}N is due to preferential escape of ^{14}N from the martian atmosphere [e.g., *McElroy et al.*, 1976; *Fox and Dalgarno*, 1983; *Fox and Hać*, 1997; *Chassefière and Leblanc*, 2004]. Some models of sputtering and photochemical escape of nitrogen to space suggest that exchange with surface/interior reservoirs is needed to buffer the nitrogen against excessive fractionation due to escape [*Jakosky et al.*, 1994; *Zent et al.*, 1994], leading to a loss of ∼ 90% of atmospheric nitrogen over time [*Jakosky and Phillips*, 2001]. The detailed history and mechanisms of exchange between atmosphere and surface/interior are poorly understood for nitrogen, compared to similar processes that fractionate atmospheric carbon and oxygen [*Webster et al.*, 2013], via exchange between polar ices, carbonates, and regolith adsorption [*Jakosky*, 1991; *Fanale et al.*, 1992].

SAM may provide insight into these processes by investigating nitrogen-containing compounds in solid samples. Reduced and oxidized compounds have tentatively been identified in evolved gases, including N, NO, HCN, CN, and CH_3CN [*Stern et al.*, 2013; *Navarro-González et al.*, 2013]. The origin of the detected nitrogen could include terrestrial sources within the SAM instrument or the Curiosity sample chain, exogenous nitrogen delivered by meteorites, or indigenous martian inorganic and organic matter. Exchange between solid and atmospheric reservoirs could occur as organic surface nitrogen is photolytically or radiolytically decomposed to N_2 or oxidized to inorganic nitrogen in the form of nitrates, which are also converted to N_2 by the current impact flux [*Manning et al.*, 2008].

Acknowledgments. The authors thank the MSL Team for successful operation of the mission, Jane Fox for a thorough and helpful review, and Bernard Marty and Guillaume Avice for insightful comments on the analysis of Tissint. This research was supported by the NASA Mars Science Laboratory Project.

References

Atreya, S.K., Squyres, S.W., Mahaffy, P.R., Leshin, L.A., Franz, H.B., Trainer, M.G., Wong, M.H., McKay, C.P., Navarro-González, R., MSL Science Team (2013), MSL/SAM Measurements of Non-Condensable Volatiles in the Atmosphere of Mars—Possibility of Seasonal Variations, *LPI Contributions*, *1719*, 2130.

Avice, G. (2012), *Analyse géochimique d'une nouvelle météorite martienne: Tissint*. Master's thesis, École Nationale Supérieure de Géologie, Vandœuvre-lès-Nancy, France.

Ballou, E.V., Wood, P.C. (1978), Chemical interpretation of Viking Lander 1 life detection experiment, *Nature*, *271*, 644–645.

Becker, R.H., Pepin, R.O. (1984), The case for a Martian origin of the shergottites—Nitrogen and noble gases in EETA 79001, *Earth and Planetary Science Letters*, *69*, 225–242.

Bogard, D.D., Johnson, P. (1983), Martian gases in an Antarctic meteorite?, *Science*, *221*, 651–654.

Chassefière, E., Leblanc, F. (2004), Mars atmospheric escape and evolution; in with the solar wind, *Planetary and Space Science*, *52*, 1039–1058.

Chennoui Aoudjehane, H., Avice, G., Barrat, J.-A., Boudouma, O., Chen, G., Duke, M.J.M., Franchi, I.A., Gattacceca, J., Grady, M.M., Greenwood, R.C., Herd, C.D.K., Hewins, R., Jambon, A., Marty, B., Rochette, P., Smith, C.L., Sautter, V., Verchovsky, A., Weber, P., Zanda, B. (2012), Tissint Martian Meteorite: A Fresh Look at the Interior, Surface, and Atmosphere of Mars, *Science*, *338*, 785–788.

Coplen, T.B., Böhlke, J.K., De Bièvre, P., Ding, T., Holden, N.E., Hopple, J.A., Krouse, H.R., Lamberty, A., Peiser, H.S., Révész, K., Rieder, S.E., Rosman, K.J.R., Roth, E., Taylor, P.D.P., Vocke, Jr., R.D., Xiao, Y.K. (2002), Isotope-Abundance Variations of Selected Elements (IUPAC Technical Report), *Pure Appl. Chem.*, *74*, 1987–2017.

Dahmen, G., Wilson, T.L., Matteucci, F. (1995), The nitrogen isotope abundance in the galaxy. 1: The galactic disk gradient, *Astronomy and Astrophysics*, *295*, 194–198.

Fanale, F.P., Jakosky, B.M. (1982), Regolith-atmosphere exchange of water and carbon dioxide on Mars—Effects on atmospheric history and climate change, *Planetary and Space Science*, *30*, 819–831.

Fanale, F.P., Postawko, S.E., Pollack, J.B., Carr, M.H., Pepin, R.O. (1992), Mars—Epochal climate change and volatile history, in *Mars*, pp. 1135–1179, Univ. Arizona Press, Tucson AZ.

Fanale, F.P., Salvail, J.R., Banerdt, W.B., Saunders, R.S., Johansen, L.A. (1982), Seasonal carbon dioxide exchange between the regolith and atmosphere of Mars—Experimental and theoretical studies, *Journal of Geophysical Research*, *87*, 10215–10225.

Fox, J.L., Hać, A. (1997), The $^{15}N/^{14}N$ isotope fractionation in dissociative recombination of N_2^+, *Journal of Geophysical Research*, *102*, 9191–9204.

Fox, J.L., Dalgarno, A. (1983), Nitrogen escape from Mars, *Journal of Geophysical Research*, *88*, 9027–9032.

Fenton, L.K., Geissler, P.E., Haberle, R.M. (2007), Global warming and climate forcing by recent albedo changes on Mars, *Nature*, *446*, 646–649.

Grotzinger, J.P., Crisp, J., Vasavada, A.R., Anderson, R.C., Baker, C.J., Barry, R., Blake, D.F., Conrad, P., Edgett, K.S., Ferdowski, B., Gellert, R., Gilbert, J.B., Golombek, M., Gómez-Elvira, J., Hassler, D.M., Jandura, L., Litvak, M., Mahaffy, P., Maki, J., Meyer, M., Malin, M.C., Mitrofanov, I., Simmonds, J.J., Vaniman, D., Welch, R.V., Wiens, R.C. (2012), Mars Science Laboratory Mission and Science Investigation, *Space Science Reviews*, *170*, 5–56.

Hoffman, J.H., Hodges, R.R., McElroy, M.B., Donahue, T.M., Kolpin, M. (1979), Composition and structure of the Venus atmosphere—Results from Pioneer Venus, *Science*, *205*, 49–52.

Jakosky, B.M. (1991), Mars volatile evolution - Evidence from stable isotopes, *Icarus*, *94*, 14–31.

Jakosky, B.M., Phillips, R.J. (2001), Mars' volatile and climate history, *Nature*, *412*, 237–244.

Jakosky, B.M., Pepin, R.O., Johnson, R.E., Fox, J.L. (1994), Mars atmospheric loss and isotopic fractionation by solar-wind-induced sputtering and photochemical escape, *Icarus*, *111*, 271–288.

Mahaffy, P.R., Webster, C.R., Cabane, M., Conrad, P.G., Coll, P., Atreya, S.K., Arvey, R., Barciniak, M., Benna, M., Bleacher, L., Brinckerhoff, W.B., Eigenbrode, J.L., Carignan, D., Cascia, M., Chalmers, R.A., Dworkin, J.P., Errigo, T., Everson, P., Franz, H., Farley, R., Feng, S., Frazier, G., Freissinet, C., Glavin, D.P., Harpold, D.N., Hawk, D., Holmes, V., Johnson, C.S., Jones, A., Jordan, P., Kellogg, J., Lewis, J., Lyness, E., Malespin, C.A., Martin, D.K., Maurer, J., McAdam, A.C., McLennan, D., Nolan, T.J., Noriega, M., Pavlov, A.A., Prats, B., Raaen, E., Sheinman, O., Sheppard, D., Smith, J., Stern, J.C., Tan, F., Trainer, M., Ming, D.W., Morris, R.V., Jones, J., Gundersen, C., Steele, A., Wray, J., Botta, O., Leshin, L.A., Owen, T., Battel, S., Jakosky, B.M., Manning, H., Squyres, S., Navarro-González, R., McKay, C.P., Raulin, F., Sternberg, R., Buch, A., Sorensen, P., Kline-Schoder, R., Coscia, D., Szopa, C., Teinturier, S., Baffes, C., Feldman, J., Flesch, G., Forouhar, S., Garcia, R., Keymeulen, D., Woodward, S., Block, B.P., Arnett, K., Miller, R., Edmonson, C., Gorevan, S., Mumm, E. (2012), The Sample Analysis at Mars Investigation and Instrument Suite, *Space Science Reviews*, *170*, 401–478.

Mahaffy, P.R., Webster, C.R., Atreya, S.K., Franz, H., Wong, M.H., Conrad, P.G., Harpold, D., Jones, J.H., Leshin, L.A., Manning, H.L.K., Owen, T., Pepin, R.O., Squyres, S., Trainer, M.G., and MSL Science Team (2013) Abundance and Isotopic Composition of Gases in the Martian Atmosphere from the Curiosity Rover, *Science*, *341*(263), 263–266.

Malin, M.C., Caplinger, M.A., Davis, S.D. (2001), Observational Evidence for an Active Surface Reservoir of Solid Carbon Dioxide on Mars, *Science*, *294*, 2146–2148.

Manning, C.V. McKay, C.P., and Zahnle, K.J. (2008), The nitrogen cycle on Mars: Impact decomposition of near-surface nitrates as a source for a nitrogen steady state, *Icarus*, *197*, 60–64.

Marti, K., Mathew, K.J. (2000), Ancient Martian nitrogen, *Geophysical Research Letters*, *27*, 1463–1466.

Marti, K., Kim, J.S., Thakur, A.N., McCoy, T.J., Keil, K. (1995), Signatures of the Martian Atmosphere in Glass of the Zagami Meteorite, *Science*, *267*, 1981–1984.

Marty, B., Chaussidon, M., Wiens, R.C., Jurewicz, A.J.G., Burnett, D.S. (2011), A ^{15}N-Poor Isotopic Composition for the Solar System As Shown by Genesis Solar Wind Samples, *Science*, *332*, 1533–1536.

McElroy, M.B., Yung, Y.L., and Nier, A.O. (1976), Isotopic composition of nitrogen: implications for the past history of Mars atmosphere, *Science*, *194*, 70–72.

Navarro-González, R., Stern, J., Sutter, B., Archer, D., McAdam, A., Franz, H.B., McKay, C.P., Coll, P., Cabane, M., Ming, D.W., Raulin, F., Brunner, A.E., Glavin, D., Eigenbrode, J.L., Jones, J.H., Freissinet, C., Leshin, L., Wong, M.H., Atreya, S.K., Wray, J.J., Steele, A., Buch, A., Prats, B.D., Szopa, C., Coscia, D., Teinturier, S., Conrad, P., Mahaffy, P., Martn-Torres, F.J., Zorzano-Mier, M.-P., Grotzinger, J.P., and the MSL Science Team (2013), Possible detection of nitrates on Mars by the Sample Analysis at Mars (SAM) instrument, *LPI Contributions*, *1719*, 2648.

Nier, A.O., McElroy, M.B. (1977), Composition and structure of Mars' upper atmosphere - Results from the neutral mass spectrometers on Viking 1 and 2, *Journal of Geophysical Research*, *82*, 4341–4349.

Niemann, H.B., Atreya, S.K., Bauer, S.J., Carignan, G.R., Demick, J.E., Frost, R.L., Gautier, D., Haberman, J.A., Harpold, D.N., Hunten, D.M., Israel, G., Lunine, J.I., Kasprzak, W.T., Owen, T.C., Paulkovich, M., Raulin, F., Raaen, E., Way, S.H. (2005), The abundances of constituents of Titan's atmosphere from the GCMS instrument on the Huygens probe, *Nature*, *438*, 779–784.

Nyquist, L.E., Bogard, D.D., Shih, C.-Y., Greshake, A., Stöffler, D., Eugster, O. (2001), Ages and Geologic Histories of Martian Meteorites, *Space Science Reviews*, *96*, 105–164.

Owen, T.C., (1992), The composition and early history of the atmosphere of Mars, in *Mars*, pp. 818–834, Univ. Arizona Press, Tucson AZ.

Owen, T., Biemann, K., Biller, J.E., Lafleur, A.L., Rushneck, D.R., Howarth, D.W. (1977), The composition of the atmosphere at the surface of Mars, *Journal of Geophysical Research*, *82*, 4635–4639.

Owen, T., Mahaffy, P.R., Niemann, H.B., Atreya, S., Wong, M.H. (2001), Protosolar Nitrogen, *The Astrophysical Journal*, *553*, L77–L79.

Oyama, V.I., Berdahl, B.J. (1977), The Viking gas exchange experiment results from Chryse and Utopia surface samples, *Journal of Geophysical Research*, *82*, 4669–4676.

Stern, J.C., Steele, A., Brunner, A.E., Coll, P., Eigenbrode, J.L., Franz, H.B., Freissinet, C., Glavin, D., Jones, J.H., Navarro-González, R., Mahaffy, P.R., McAdam, A.C., McKay, C.P., Wray, J., MSL Science Team (2013), Detection of Reduced Nitrogen Compounds at Rocknest Using the Sample Analysis at Mars (SAM) Instrument on the Mars Science Laboratory (MSL), *LPI Contributions*, *1719*, 2790.

Schwenzer, S.P., Herrmann, S., Mohapatra, R.K., Ott, U. (2007), Noble gases in mineral separates from three shergottites: Shergotty, Zagami, and EETA79001, *Meteoritics and Planetary Science*, *42*, 387–412.

Trainer, M.G., McKay, C.P., Franz, H.B., Wong, M.H., Mahaffy, P.R., Atreya, S.K., Manning, H.L.K., Conrad, P.G., Brunner, A.E., Malespin, C.A., Owen, T.C., Pepin, R.O., Navarro-González, R., and MSL Science Team (2013), Change in the 40Ar/N of the Mars Atmosphere from Viking to MSL: A possible indication of climate change on Mars, *AGU Fall Meeting*.

Webster, C.R., Mahaffy, P.R., Flesch, G.J., Niles, P.B., Jones, J.H., Leshin, L.A., Atreya, S.K., Stern, J.C., Christensen, L.E., Owen, T.C., Franz, H.B., Pepin, R.O., Steele, A., and the MSL Science Team (2013), Isotope Ratios of H, C, and O in CO_2 and H_2O of the Martian Atmosphere, *Science*, *341*, 260–263.

Wiens, R.C., Becker, R.H., Pepin, R.O. (1986), The case for a Martian origin of the shergottites. II - Trapped and indigenous gas components in EETA 79001 glass, *Earth and Planetary Science Letters*, *77*, 149–158.

Wong, M.H., Mahaffy, P.R., Atreya, S.K., Niemann, H.B., Owen, T.C. (2004), Updated Galileo probe mass spectrometer measurements of carbon, oxygen, nitrogen, and sulfur on Jupiter, *Icarus*, *171*, 153–170.

Wong, M.H., Atreya, S.K., Mahaffy, P.R., Trainer, M., Franz, H., Stern, J., Owen, T., McKay, C.P., Jones, J.H., Manning, H., Navarro-González, R. (2013), MSL/SAM Measurements of Nitrogen and Argon Isotopes in the Mars Atmosphere, *LPI Contributions*, *1719*, 1712. LPSC E-Poster at http://www.lpi.usra.edu/meetings/lpsc2013/eposter/1712.pdf.

Zent, A.P., Quinn, R.C., Jakosky, B.M. (1994), Fractionation of nitrogen isotopic on Mars: The role of the regolith as a buffer, *Icarus*, *112*, 537–540.

York, D., Evensen, N.M., Martínez, M.L., de Basabe Delgado, J. (2004), Unified equations for the slope, intercept, and standard errors of the best straight line, *American Journal of Physics*, *72*, 367–375.

Corresponding author: Michael H. Wong, Department of Atmospheric, Oceanic, and Space Sciences, University of Michigan, Space Research Building, 2455 Hayward Street, Ann Arbor MI 48109-2143, USA. (mike.wong@umich.edu)

WONG ET AL. [2013]: MARS ATMOSPHERIC NITROGEN ISOTOPES

SUPPLEMENTARY MATERIAL

1. Definitions

We define the following isotopic and ionization fractions:

- α = the ratio of $^{14}N/^{15}N$. This is the unknown in the Mars sample.
- $\beta = \frac{N^+ \text{ions}}{N^+ + N_2^{++} \text{ions}}$ produced from N_2.
- $\gamma = \frac{N_2^{++} \text{ions}}{N^+ + N_2^{++} \text{ions}}$ produced from N_2.

Then $\beta + \gamma = 1$, and β/γ is the N^+/N_2^{++} splitting fraction.

Additional definitions:

- $P(X)$ = the probability that one atom or molecule, drawn at random from a given sample, is a member of species X.
- $n(X)$ = the number of atoms or molecules of species X in the sample.

2. Distribution of N isotopes in a molecular population

For a population of nitrogen molecules, we have to determine how they are partitioned into the three isotopologues of $^{14}N_2$, $^{15}N_2$, and $^{14}N^{15}N$ (for convenience, we can also call these $^{28}N_2$, $^{30}N_2$, and $^{29}N_2$ respectively).

It is possible that there is some fractionation, so that ^{15}N is preferentially (rather than randomly) partitioned among $^{30}N_2$ and $^{29}N_2$. But we assume that N-exchange between molecules is faster than any loss mechanism that fractionates nitrogen.

The sample consists of N_2 molecules, but we can select just a single atom from this population first. The probability that we selected an atom of ^{14}N is given by

$$P(^{14}\mathrm{N}) = \frac{n(^{14}\mathrm{N})}{n(^{14}\mathrm{N}) + n(^{15}\mathrm{N})} = \frac{\alpha}{\alpha + 1}. \tag{1}$$

Similarly,

$$P(^{15}\mathrm{N}) = \frac{1}{\alpha + 1}. \tag{2}$$

Because this is a population of molecules, the atom we just selected actually has another atom dangling off of it. Probabilities can just be multiplied, so the probabilities for selecting the homoisotopic molecules are easily derived:

$$P(^{28}\mathrm{N}_2) = P(^{14}\mathrm{N}^{14}\mathrm{N}) = P(^{14}\mathrm{N})P(^{14}\mathrm{N}) = \frac{\alpha^2}{(\alpha + 1)^2}. \tag{3}$$

$$P(^{30}\mathrm{N}_2) = P(^{15}\mathrm{N})P(^{15}\mathrm{N}) = \frac{1}{(\alpha + 1)^2}. \tag{4}$$

But for the heteroisotopologue $^{29}N_2$, there are two substitution sites. So,

$$P(^{29}\mathrm{N}_2) = P(^{14}\mathrm{N}^{15}\mathrm{N}) + P(^{15}\mathrm{N}^{14}\mathrm{N}) = 2P(^{14}\mathrm{N})P(^{15}\mathrm{N}) = \frac{2\alpha}{(\alpha + 1)^2} \tag{5}$$

Everywhere except for Eqn. 5, we will consider $^{14}N^{15}N$, $^{15}N^{14}N$, and $^{29}N_2$ to be identical. Taking the ratio of Eqns. 3 and 5 shows that $^{28}N_2/^{29}N_2$ is a factor of two different from $^{14}N/^{15}N$.

3. Determination of splitting fractions and isotope ratios from SAM QMS data

In AS-DIRECT for samples at full atmospheric pressure, m/z 28 is saturated, and both m/z 28 and 29 have contributions from CO and CO_2. There are lots of counts at m/z 15, but this is largely due to a strong instrumental hydrocarbon background, making it very difficult to reliably separate the signal from the background. But there ARE counts at m/z 14 and 14.5, well above the background level.

The m/z 14/14.5 count ratio also gives the best signal/background level in enrichment experiments.

At m/z 14.5, only $^{29}N_2^{++}$ is present. But at m/z 14, two sources contribute: $^{14}N^+$ and $^{28}N_2^{++}$. The $^{14}N^+$ ions come from both $^{28}N_2$ and $^{29}N_2$.

The probability of measuring a particular daughter ion depends on the the probability of starting with the right parent ion and the splitting fractions β and γ. At m/z 14.5,

$$P(^{29}\mathrm{N}_2^{++}) = P(^{29}\mathrm{N}_2)P(\mathrm{N}_2 \rightarrow \mathrm{N}_2^{++}) = \frac{2\gamma\alpha}{(\alpha+1)^2}. \tag{6}$$

At m/z 14, there are more terms because both singly and doubly charged ions contribute, and both $^{28}\mathrm{N}_2$ and $^{29}\mathrm{N}_2$ are parent ions:

$$\begin{aligned} P(^{28}\mathrm{N}_2^{++}) + P(^{14}\mathrm{N}^{+}) &= P(^{28}\mathrm{N}_2)P(\mathrm{N}_2 \rightarrow \mathrm{N}_2^{++}) \\ &\quad + P(^{28}\mathrm{N}_2)P(\mathrm{N}_2 \rightarrow \mathrm{N}^{+}) + P(^{29}\mathrm{N}_2)\frac{P(\mathrm{N}_2 \rightarrow \mathrm{N}^{+})}{2} \\ &= \frac{\gamma\alpha^2}{(\alpha+1)^2} + \frac{\beta\alpha^2}{(\alpha+1)^2} + \frac{\beta\alpha}{(\alpha+1)^2} \end{aligned} \tag{7}$$

Then dividing Eqn. 7 by Eqn. 6 gives the observable ratio of m/z 14/14.5 (which we denote by [m14/m14.5]):

$$\left[\frac{\mathrm{m14}}{\mathrm{m14.5}}\right] = \frac{\gamma\alpha^2 + \beta\alpha^2 + \beta\alpha}{2\gamma\alpha} = \frac{(1-\beta)\alpha^2 + \beta\alpha^2 + \beta\alpha}{2(1-\beta)\alpha}. \tag{8}$$

For a calibration experiment, where we have a known $^{14}\mathrm{N}/^{15}\mathrm{N}$ ratio α, we can solve Eqn. 8 for β to determine the N^+/m14 splitting fraction:

$$\beta = \frac{2\left[\frac{\mathrm{m14}}{\mathrm{m14.5}}\right] - \alpha}{2\left[\frac{\mathrm{m14}}{\mathrm{m14.5}}\right] + 1}. \tag{9}$$

Or, for a flight experiment, we can derive the unknown $^{14}\mathrm{N}/^{15}\mathrm{N}$ ratio with knowledge of SAM's N^+ splitting fraction β:

$$\alpha = 2(1-\beta)\left[\frac{\mathrm{m14}}{\mathrm{m14.5}}\right] - \beta. \tag{10}$$

On 2013-01-08, Jen Stern measured $\delta^{15}\mathrm{N}$ in the SAM FM cal gas cell to be -0.587 ± 0.014 per mil, or $\alpha = 272.195 \pm 0.003$. This allowed a determination of $\beta = 0.404 \pm 0.033$ from the combination of one SAM testbed experiment and four pre-flight calibration experiments. This measurement of β was presented at the 2013 LPSC [*Wong et al.* 2013].

4. Nitrogen isotopic ratio: error budget

Uncertainties are discussed briefly in the main text. The uncertainties in Fig. S1 are ESTIMATES of the true errors. For simplicity, we do not present uncertainties in the uncertainty estimates, but the uncertainty estimates are judged to be accurate to within 50% of their values. The uncertainty in the correct background correction is particularly

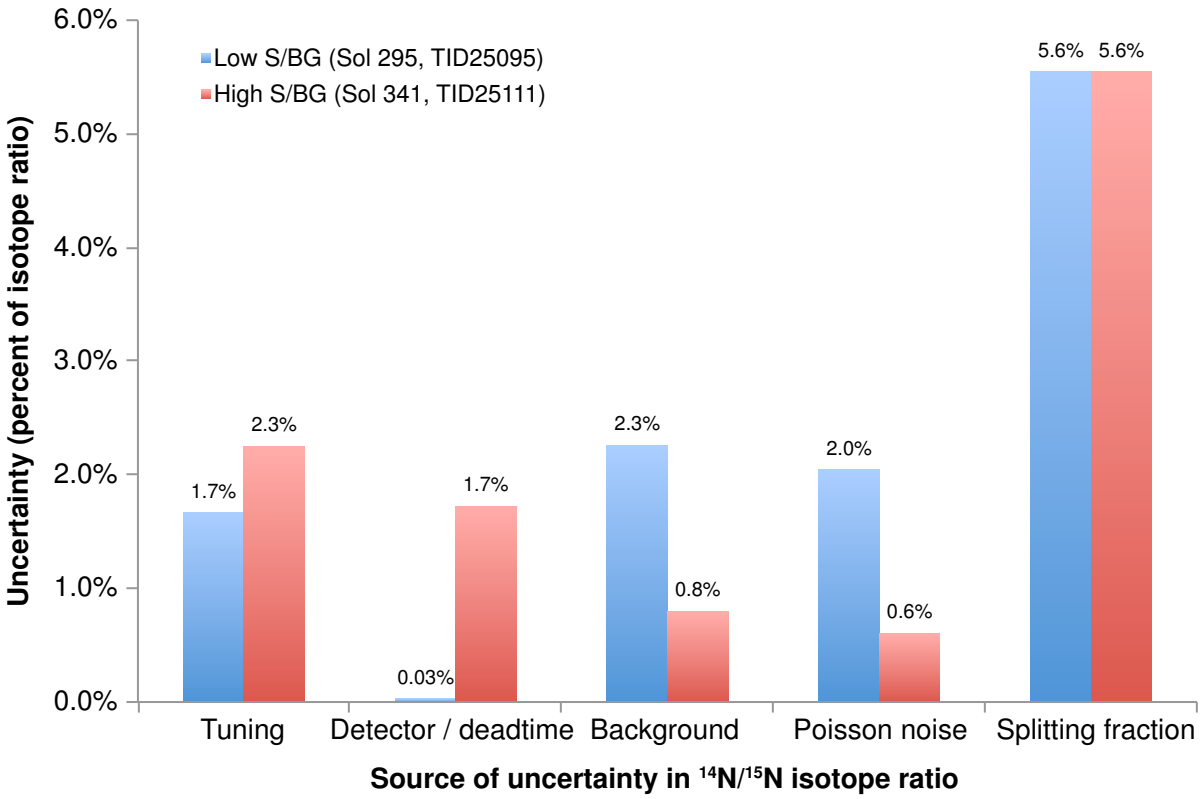

FIGURE S1. Error budget for the $^{14}N/^{15}N$ isotope ratios measured by MSL/SAM. Typical high and low S/BG cases are shown (see Table 1 in the main text).

difficult to estimate, since it is not possible to simultaneously measure both background and sample.

The individual sources of error evaluated for these measurements are:

- Tuning: QMS peak shapes are flat-topped functions, but are not perfectly flat. The most reliable number to use for count ratios is the peak counting rate at for each mass to charge ratio, but due to instrument tuning constraints, the peak shape functions sometimes have offset in their maxima. For example, Fig. 1 in the main text shows the peak counts/sec for m/z 14 occurs at m/z 13.8 rather than m/z 14.0. We use peak shape templates to normalize m/z 14 data to the peak counts/sec; without this adjustment, tuning errors are approximately twice as large. An accurate tuning correction for the m/z 14.5 data is not available because the wings of the peak are hidden by signal from m/z 14 and 15. Tuning

variation is currently being characterized by the team, and depends on factors such as instrument temperature. Tuning variation is not apparently correlated to count rates.

- Detector/deadtime: Detector effects are corrected to remove nonlinearity from the signal at high counting rates. For low count rates, the correction is extremely small. For count rates over a million counts/sec, the correction becomes significant at the 1-5% level.

- Background: Background corrections are challenging, and the SAM team continues to refine our methods for this correction. We have estimated the background correction uncertainty by comparing alternate corrections using different tracer masses and fitting techniques. The bar graph clearly shows that background uncertainty is reduced in the enrichment run with high S/BG.

- Noise: Noise in the SAM QMS follows a Poisson distribution, as expected for counting detectors [*Bevington and Robinson* 1992]. The relative contribution from this uncertainty source is reduced at higher count rates (because the uncertainty on a single measurement is the square root of the counts per integration period), and also reduced by taking measurements over a longer time period. For this error budget, we show the uncertainty due to errors following a precise Poisson distribution. Errors calculated self-consistently from the data are not significantly larger, unless time-variable effects are significant.

- Splitting fraction: The uncertainty in β is not affected by data considerations such as count rates or S/BG ratios. To reduce uncertainty in this factor, high-precision measurements must be conducted on gases with known nitrogen isotopic composition. Only a limited number of calibration experiments were done with the SAM flight model before launch, and all of these experimental results are included in the determination of the splitting pattern [*Wong et al.* 2013]. However, additional experiments can be conducted on the SAM testbed, currently operating at NASA GSFC. With the flight instrument, an improvement could be achieved by measuring on-board calibration gas cell samples on Mars (after enrichment, to eliminate CO^+ signal at m/z 28).

5. δ^{15}N vs. experimental signal/BG ratio

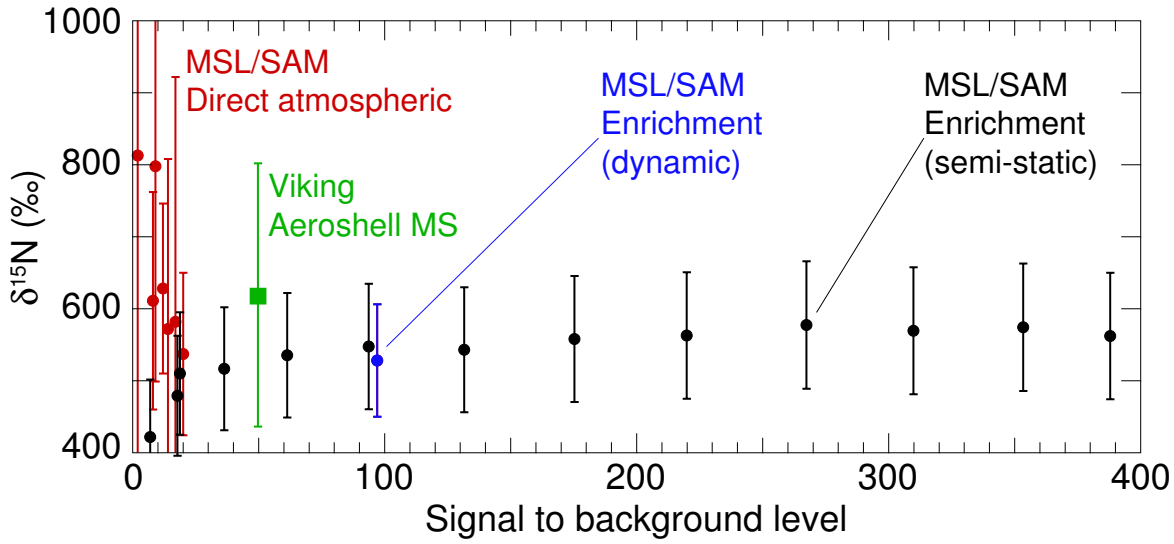

FIGURE S2. Stable δ^{15}N at different S/BG levels indicates that the background correction is not significant in the enrichment experiments. The largest single source of uncertainty at high S/BG is the uncertainty in splitting fraction β. Experiment sol numbers are given in Table 1.

6. Supplemental references

Bevington, P.R., and D.K. Robinson (1992), *Data Reduction and Error Analysis for the Physical Sciences*, WCB/McGrawHill, Dubuque, IA.